Energy transfer of highly vibrationally excited naphthalene. II. Vibrational energy dependence and isotope and mass effects

Chen-Lin Liu,[a] Hsu Chen Hsu,[b] Yuan Chin Hsu,[a] and Chi-Kung Ni[a),c)]
Institute of Atomic and Molecular Sciences, Academia Sinica, P.O. Box 23-166, Taipei, 10617 Taiwan

(Received 6 November 2007; accepted 24 January 2008; published online 31 March 2008)

The vibrational energy dependence, H and D atom isotope effects, and the mass effects in the energy transfer between rare gas atoms and highly vibrationally excited naphthalene in the triplet state were investigated using crossed-beam/time-sliced velocity-map ion imaging at various translational collision energies. Increase of vibrational energy from 16 194 to 18 922 cm^{-1} does not make a significant difference in energy transfer. The energy transfer properties also remain the same when H atoms in naphthalene are replaced by D atoms, indicating that the high vibrational frequency modes do not play important roles in energy transfer. They are not important in supercollisions either. However, as the Kr atoms are replaced by Xe atoms, the shapes of energy transfer probability density functions change. The probabilities for large translation to vibration/rotation energy transfer ($T \rightarrow VR$) and large vibration to translation energy transfer ($V \rightarrow T$) decrease. High energy tails in the backward scatterings disappear, and the probability for very large vibration to translation energy transfer such as supercollisions also decreases. © *2008 American Institute of Physics*.
[DOI: 10.1063/1.2868753]

I. INTRODUCTION

The collision dynamics of gas-phase molecules with high levels of internal energy are a key feature in many important chemical processes, such as unimolecular reactions and atmospheric photochemistry. In thermal unimolecular reactions, the energies needed for reaction are accumulated via collisions with bath atoms or molecules, whereas in recombination reactions and various photochemical processes, collisions can stabilize these highly excited intermediate species.

Early gas-phase experiments from unimolecular rate coefficients in the low-pressure and falloff regions indicated that average energy transfer in each collision is very small.[1] Recently, experimental techniques have been developed to measure fundamental energy transfer properties of highly vibrationally excited polyatomic molecules directly. They confirmed the suggestion from unimolecular reaction rate measurement.[2,3] Despite the wealth of energy transfer studies of highly vibrationally excited molecules, most experiments yield averaged quantities such as the first and second moments (i.e., $\langle \Delta E \rangle$ and $\langle \Delta E^2 \rangle$) of $P(E',E)$. Only scarce information on the collisional energy transfer probability density function $P(E',E)$ was provided experimentally.[4–13] Consequently, this is a major bottleneck in these experiments. Experiments that provide for a direct determination of $P(E',E)$ as a function of ΔE are needed for a more complete understanding of energy transfer processes.

In the past few years, extensive classical trajectory calculation has been performed in the collisional energy transfer of highly vibrationally excited molecules.[14–26] The calculation indicates how the energy transferred per collision depends on the internal energy of polyatomic molecules, on the intermolecular potential, on the mass of the bath, on the duration of collision, on the minimal distance of approach, on the relative velocity, on the vibrational modes, and on the rotation of polyatomic molecules. The calculations also provide the energy transfer probability density function directly. Some experimental results are available for comparison with the calculations. For example, experiments using transient UV absorption and IR emission techniques demonstrated the internal energy dependence of average transferred energy.[27–32] The vibration energy relaxation of azulene by He, Ne, Ar, Kr, and Xe in a thermal system showed the mass effects, the average energy transfer of which increases from He, Ne, and Ar to Kr but levels off from Kr to Xe.[27,31] Collisional deactivation of highly vibrationally excited gas-phase toluene, toluene-d_8, benzene, and benzene-d_6 investigated by Toselli and Barker demonstrated that the deuteration effects in average energy transfer is small.[33]

Recently, our crossed-beam experiments provide another alternative experimental observation for comparison with the calculations.[34–38] The advantages of the crossed-beam experiments are that collisions are controlled to occur under a specific initial conditions, i.e., under single collision conditions at a given collision energy and at very low rotational temperature (<2 K). The energy transfer probability density functions are obtained directly from the measurement. Instead of the average over thermal velocity distribution and rotational distribution, calculations in such specific conditions are more sensitive to any adjustable parameter when they are compared to the crossed-beam experimental

[a)]Also at the Department of Chemistry, National Tsing Hua University, Hsinchu 30013, Taiwan.
[b)]Also at the Department of Chemistry, National Taiwan University, Taipei 10617, Taiwan.
[c)]Author to whom correspondence should be addressed. Electronic mail: ckni@po.iams.sinica.edu.tw.

TABLE I. Velocity uncertainties and speed ratios of naphthalene molecular beam. ΔV_x and ΔV_y are the full widths at half maximum of the naphthalene velocity distribution in the x and y directions, respectively. V_{nap} is the naphthalene velocity in the laboratory frame, U_{nap} is the naphthalene velocity in the center-of-mass frame, $\Delta V=(\Delta V_x+\Delta V_y)/2$, $\pm E_{coll}$ is the uncertainty of collision energy, and $\pm\Delta E_{coll}=E_{coll}(\Delta V/U_{nap})$.

E_{coll} (cm^{-1})[a]	105[b]	422[b]	585[b]	847[b]	564(d_8)[b]	853(d_8)[b]	463[c]	891[c]	1005[c]
ΔV_x (pixel)	0.9	2.9	2.0	4.0	2.6	2.4	1.4	3.5	3.4
ΔV_y (pixel)	1.7	2.8	2.6	5.6	3.1	5.8	1.4	3.6	47
$V_{nap}/\Delta V$	63	29	51	23	33	23	54	33	26
$U_{nap}/\Delta V$	14.5	13	18.7	11	15	12.5	31	17	16
$\pm\Delta E_{coll}$ (cm^{-1})	7	32	31	77	38	68	15	52	63

[a]Collision energy.
[b]Collision with Kr.
[c]Collision with Xe.

results.[39–41] Therefore, the comparison provides the opportunity to understand the details of the energy transfer mechanism. In this work, we investigated the mass effects, H and D atom isotope effects, and the vibrational energy dependence in the energy transfer between Kr and Xe atoms and highly vibrationally excited naphthalene in the triplet state using crossed-beam techniques.

II. EXPERIMENT

The details of the experiment have been described in previous studies.[33–37,42,43] Only a brief description is described here. The experimental apparatus included a pulsed UV laser set at 248 or 266 nm, one VUV laser at 157 nm, a differentially pumped crossed molecular beam vacuum chamber, and a time-of-flight mass spectrometer with a time-sliced velocity-map ion imaging system. The rotationally cold naphthalene molecular beam was formed by flowing carrier gas at a pressure of 2850 Torr through a reservoir filled with naphthalene at ~340 K. Carrier gases included ultrapure (99.999%) Kr, Ar, Ne, He, or the mixtures of these gases for the different collision energies. The mixture of naphthalene and carrier gas was then expanded through a nozzle maintained at the temperature of 400 K to form a rotationally cold naphthalene beam. After passing two skimmers and entering into the main chamber, naphthalene molecules in the molecular beam were excited to the S_2 state by UV photons. Most naphthalene molecules (93%) become highly vibrationally excited in the triplet state after intersystem crossing.[44–47] About 20–30 μs after photoexcitation, these highly vibrationally excited naphthalene in the triplet state flew into the collision region and collided with gas atoms from an atomic beam. The nozzle for the atomic beam maintained at 450 K to avoid clusters. The scattered naphthalene molecules were then ionized by 157 nm photons and the velocity distributions of these naphthalene cations were measured by a time-sliced velocity-map ion imaging system. Note that the 157 nm photon energy is only large enough to ionize naphthalene in the triplet state. It is not large enough to ionize the unexcited naphthalene or the naphthalene in the ground state after internal conversion.

From the conservation of linear momentum in the center-of-mass frame, once the naphthalene final velocity is measured, we can obtain the final velocity of the corresponding scattered atom. From both final velocities, the total final translational energy can be calculated. In addition, the initial velocity distributions of both naphthalene and atomic beams are very narrow and well defined, as listed in Table I; thus we can obtain the initial total translational energy from the molecular beam velocities. The initial internal energy is the UV photon energy, which is also known precisely. Since we know the initial translational energy E_{trans}, initial internal energy E_{int}, and final translational energy E'_{trans}, the final internal energy, and therefore the amount of transferred energy, can be obtained from the conservation of total energy, $E_{int}+E_{trans}=E'_{int}+E'_{trans}$.

III. RESULTS AND DISCUSSION

Since the details of data analysis have been described in a previous study, only the final results are presented here.

A. Vibrational energy dependence

Figure 1 shows the angular resolved energy transfer probability density functions of naphthalene excited by 266 and 248 nm at three different collision energies. For each wavelength at each collision energy, the angular resolved probability density function (double differential cross section with respect to solid angle Ω and transferred energy ΔE) was normalized so that $\int\int(d^2\sigma/d\Omega d\Delta E)d\Omega d\Delta E=1$. The vibrational energy changes from 16 194 to 18 922 cm^{-1} as the pump wavelength changes from 266 to 248 nm. However, the shapes and magnitudes of the density functions for translation (T) → vibration/rotation (VR) up collisions as well as vibration (V) → translation (T) down collisions are almost identical at these two wavelengths. In addition, we paid special attention on the high energy tails of the density functions. As shown in Figs. 1(c), 1(f), and 1(i), the probability of large energy transfer, such as supercollisions, does not change with the pump wavelength.

In Fig. 1, the total cross section was normalized to be 1 separately for each wavelength so that we can compare the shapes of energy transfer probability density functions for different vibrational energies. In order to compare the ratio of absolute magnitudes of the energy transfer probability density functions without normalization, the curves in Fig. 1 need to be scaled so that the area under each curve is proportional to the relative absolute total collision cross sections. The ion image intensity S_{image} is proportional to the absolute total collision cross section σ_{coll}, intensity of rare gas beam, I_{rare}, intensity of naphthalene in the triplet state,

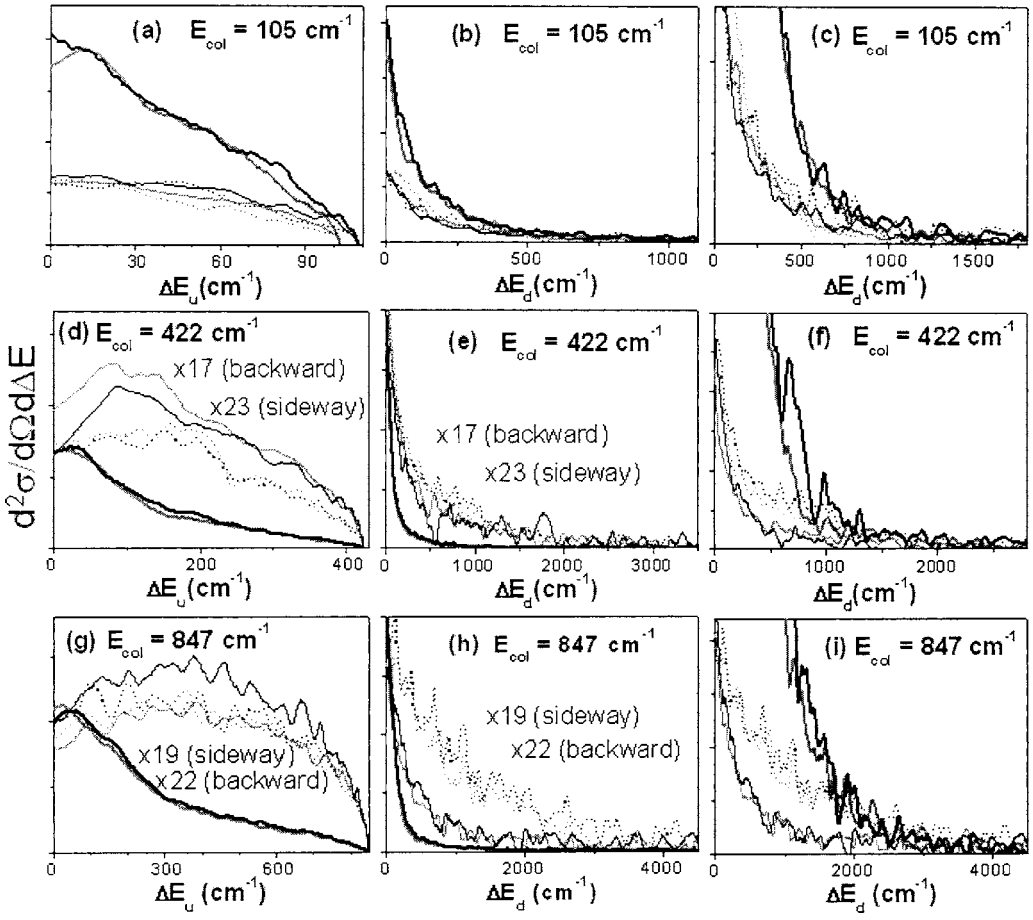

FIG. 1. Angular resolved energy transfer probability density functions (double differential cross section with respect to solid angle and transferred energy) of naphthalene excited by 266 and 248 nm in collisions with Kr at various collision energies. Thick black line, thin black line, and dot black line represent near forward, sideway, and backward density functions excited by 248 nm; thick gray line, thin gray line, and dot gray line represent near forward, sideway, and backward density functions excited by 266 nm. The first column represents the up collisions $T \rightarrow VR$ energy transfer; the second column represents the down collisions $V \rightarrow T$ energy transfer. The third column shows the region of maximum down collisions $V \rightarrow T$ energy transfer. The density functions at each collision energy for each pump wavelength are normalized separately so that $\int\int (d^2\sigma/d\Omega d\Delta E) d\Omega d\Delta E = 1$. In each plot, the density functions for 266 and 248 nm are plotted in the same scale.

I_{nap*}, the ionization cross section of naphthalene in the triplet state by 157 nm photons, σ_{157} and the 157 nm laser intensity I_{157}:

$$S_{image} \propto I_{rare} I_{nap*} \sigma_{coll} \sigma_{157} I_{157}. \tag{1}$$

I_{nap*} is proportional to the naphthalene molecular beam intensity, UV absorption cross section, and UV laser intensity. In addition to the measurement of ion image intensity when excited naphthalene collided with rate gases, we also measured the naphthalene ion intensity without rare gas atomic beam. The naphthalene ion intensity measured in such conditions is simply proportional to the naphthalene in the triplet state, ionization cross section at 157 nm, and 157 nm laser intensity:

$$S_{ion} \propto I_{nap*} \sigma_{157} I_{157}. \tag{2}$$

Combine Eqs. (1) and (2), the absolute total collision cross section can be expressed by the following equation:

$$\sigma_{coll} \propto \frac{S_{image}}{S_{ion}} \frac{1}{I_{rare}}. \tag{3}$$

These equations show that UV laser intensity, UV absorption cross section, VUV laser intensity, and VUV ionization cross section are all combined into a simple measurement, i.e., S_{ion}. This largely reduced the uncertainty in the measurement of each parameter. The ratio of absolute total cross sections at 266 and 248 nm can be expressed by the following equation:

$$r = \frac{\sigma_{coll}(248\ \text{nm})}{\sigma_{coll}(266\ \text{nm})} = \frac{\dfrac{S_{image}(248\ \text{nm})}{S_{ion}(248\ \text{nm})} \dfrac{I_{rare}(266\ \text{nm})}{I_{rare}(248\ \text{nm})}}{\dfrac{S_{image}(266\ \text{nm})}{S_{ion}(266\ \text{nm})}}. \tag{4}$$

During the experimental measurement for different UV wavelengths, we kept the rare gas atomic beam operated under the same conditions. The UV laser beam positions, beam sizes, and delay times for different wavelengths also remained the same. Meanwhile, we measured the ion image intensity S_{image} and ion intensity S_{ion} for different UV wavelength alternatively at least five times. The result shows that

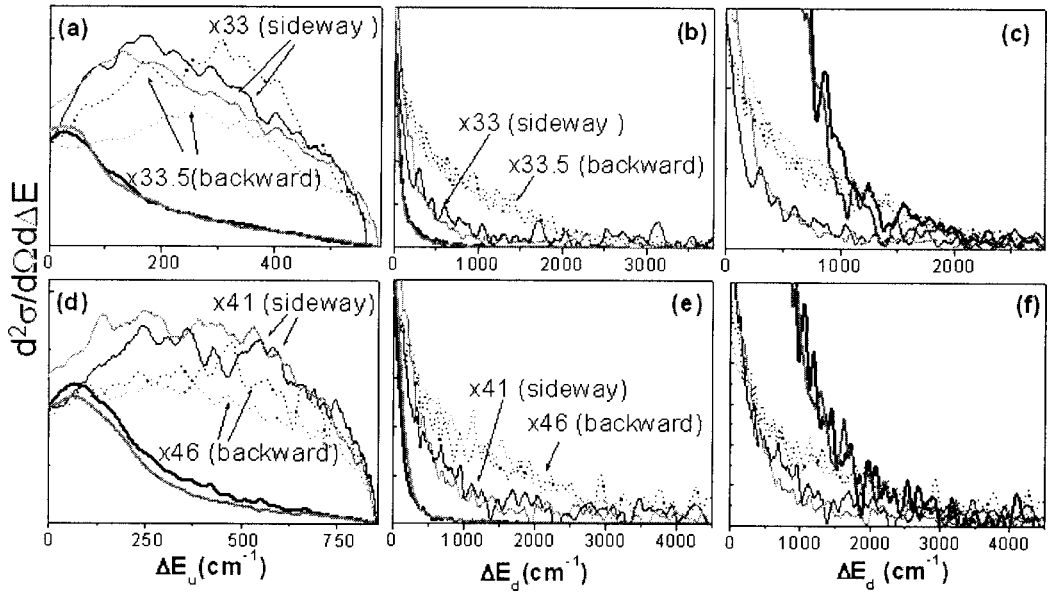

FIG. 2. Angular resolved energy transfer probability density functions for naphthalene-h_8 and naphthalene-d_8 in collisions with Kr at two collision energies. Thick black line, thin black line, and black dot line represent near forward, sideway, and backward density functions for naphthalene-d_8; thick gray line, thin gray line, and gray dot line represent near forward, sideway, and backward density functions for naphthalene-h_8. Collision energies are 564 and 585 cm^{-1} for naphthalene-d_8 and naphthalene-h_8, respectively, in (a)–(c); they are 853 and 848 cm^{-1} for d_8-naphthalene and h_8-naphthalene, respectively, in (d)–(f). The first column represents the up collisions T→VR energy transfer; the second column represents the down collisions V→T energy transfer. The third column shows the region of maximum down collisions V→T energy transfer. Both naphthalene-d_8 and naphthalene-d_8 are excited by 248 nm photons. The density functions at each collision energy are normalized so that $\int\int(d^2\sigma/d\Omega d\Delta E)d\Omega d\Delta E=1$. In each plot, naphthalene-d_8 and naphthalene-h_8 are plotted in the same scale.

the ratio of absolute total collision cross sections for Kr and naphthalene excited by 248 and 266 nm photons is 1.02 ± 0.04. As a result, we can conclude that naphthalene molecules with vibrational energies of 16 194 and 18 922 cm^{-1} not only have the same shapes of energy transfer probability density functions but also have the same total cross sections within our experimental uncertainty.

B. H and D atom isotope effects

Naphthalene-h_8 and naphthalene-d_8 were studied in order to investigate the roles of high vibrational frequency modes in energy transfer. Figure 2 shows the energy transfer probability density functions for two collision energies when the pump wavelength was set at 248 nm. They were also normalized at each collision energy for naphthalene-h_8 and naphthalene-d_8, respectively. Except for a small difference in the backward and sideway scatterings, as shown in Figs. 2(a) and 2(d), all the other probability density functions are very similar. The results suggest that the high vibrational frequency modes do not play an important role in the energy transfer. They do not have significant contribution in the supercollisions either.

The energy transfer probability density functions shown in Fig. 2 are normalized individually. They are useful when we compare the shapes of the density functions. In order to compare the relative magnitudes of the absolute collision cross sections, a similar method described in the previous section was used to obtain the relative total collision cross sections. Here, naphthalene and naphthalene-d_8 were mixed in the same molecular beam. The measurements were performed by changing the mass gate of time of flight between $m/z=128$ for naphthalene-h_8 and $m/z=136$ for naphthalene-d_8 alternatively. The result shows that the ratio of absolute total collision cross sections for naphthalene-h_8 and naphthalene-h_8 is 1.0 ± 0.1. Consequently, we can conclude that naphthalene-h_8 and naphthalene-d_8 not only have the same energy transfer probability density functions but also have the same total cross sections.

The deuteration effects of toluene-d_8 and benzene-d_6 have been investigated by Toselli and Barker using time-resolved infrared fluorescence techniques.[33] They showed that the effects in the average energy transfer are small, but no details of the effects in the energy transfer density functions or on the supercollisions have been measured. On the other hand, the classical trajectory study on Xe colliding with highly excited azulene by Clarke *et al.* shows that the rare supercollisions occur when a hydrogen atom is compressed between the bath gas and part or all of the carbon framework.[48] This produces a strong repulsion between the Xe and H as the relative coordinate is driven high up the repulsive wall. If vibrational phases or rotation of the substrate framework are such that the bath gas and substrate separate during this compression, the final energy transfer is large. This kind of mechanism must closely relate to the C–H stretches. However, in this study, we showed that the deuteration has no effects in the energy transfer probability density functions. They are not important in supercollisions either. This is consistent with most of the theory that only the low vibrational frequency modes are important in energy transfer and supercollisions.

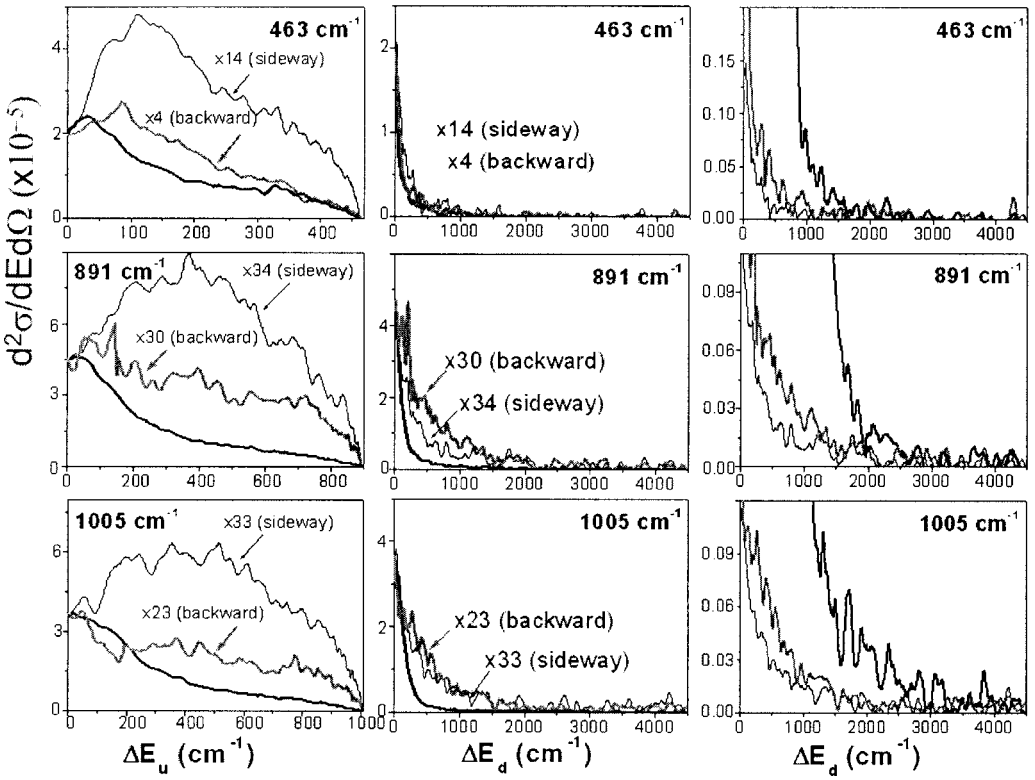

FIG. 3. Angular resolved energy transfer probability density functions of naphthalene excited by 266 nm in collisions with Xe at various collision energies. Thick black line, thin black line, and gray line represent near forward, sideway, and backward probability density functions. The first column represents the up collisions T→VR energy transfer; the second column represents the down collisions V→T energy transfer. The third column shows the region of maximum down collisions V→T energy transfer. The density functions at each collision energy are normalized separately so that $\int\int(d^2\sigma/d\Omega d\Delta E)d\Omega d\Delta E=1$.

C. Mass effects

Average energy transfer of highly vibrationally excited molecules changes as the bath atoms change from He, Ne, and Ar to Kr and Xe. This so-called mass effect has been studied in a thermal system.[27,32,44–46] For example, in the energy relaxation of highly vibrationally excited azulene, it has been shown that the average energy transfer is small for bath gas He. However, it increases rapidly for bath gases Ne and Ar. The increase from Ar to Kr is small, and then the value does not change or slightly decreases from Kr to Xe.[27,31] Similar phenomena were also observed from the highly vibrationally excited toluene[49] and cycloheptatriene.[50] Various energy transfer models were proposed to explain the "level-off effects:" the curves that average energy transfers are plotted versus mass show increase from He to Kr and then level off for the heavy atoms such that $\langle\Delta E\rangle$ for Xe is equal or less than that of Kr.

Figure 3 shows the angular resolved energy transfer probability density functions for naphthalene in collisions with Xe. In general, these distributions share many similar characteristics with the distributions in collisions with Kr. However, some differences were also observed. First, the maximum values of V→T energy transfer are smaller than those in collisions with Kr at the same collision energy. For example, the maximum values for V→T energy transfer almost reach 2000 and 3000 cm^{-1} in the collisions with Kr at collision energies of 421 and 847 cm^{-1}, respectively. Both backward and forward scatterings have contribution in the large V→T energy transfer. However, the maximum values decrease a little in collisions with Xe at the same collision energies. In addition, only the forward scatterings make the major contribution in large V→T energy transfer. The high energy tails in the backward scatterings disappear when Kr is replaced by Xe. Second, the shapes of sideway and backward scatterings for T→VR energy transfer are very similar in the collisions with Kr, but they are very different in the collisions with Xe. Finally, only small differences are found in the shapes of total energy transfer probability density functions. The total energy transfer probability density functions for Xe, as shown in Fig. 4, were obtained directly from the summation of the probability distribution functions at the

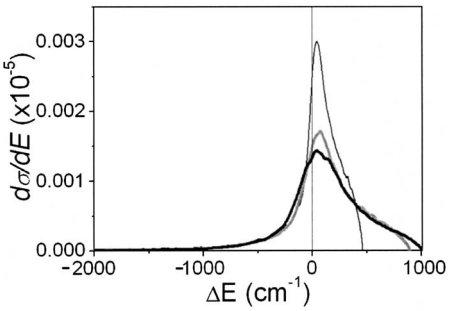

FIG. 4. Energy transfer probability density functions in collisions with Xe at various collision energies. Thin black line: 463 cm^{-1}; gray line: 891 cm^{-1}; thick black line: 1005 cm^{-1}. Negative values represent down collisions V→T energy transfer and positive values represent up collisions T→VR energy transfer. The density functions at each collision energy are normalized separately so that $\int(d\sigma/d\Delta E)d\Delta E=1$.

various scattering angles. A small portion of the image in the forward direction was blocked by the stainless steel pin ($\theta < \pm 10°$ and $\Delta E_u < 350$ cm^{-1} and $\Delta E_d < 400$ cm^{-1}). Linear extrapolation was made from large scattering angles to this region. Since the angle outside the blocked forward region, i.e., $\theta > \pm 10°$, also has contribution in the energy transfer regions $\Delta E_u < 350$ cm^{-1} and $\Delta E_d < 400$ cm^{-1}, the extrapolation for the small portion in forward scatterings only increases the probability by 10%–20% in the small energy transfer region. The increase is the difference between the intensity zero and the intensity from linear extrapolation in the blocked forward region. Even though the actual distribution maybe different from the linear extrapolation, the change of density function due to the difference from linear extrapolation is not likely to be larger than the difference between values of zero and linear extrapolation. As a result, Fig. 4 provides reliable probability density functions. Compared to those density functions in collisions with Kr, we found that the major difference is in the region of small energy transfer. However, this is the region where linear extrapolation was made.

In principle, the relative total cross sections between Kr and Xe can be obtained from the method described above. In reality, since Kr and Xe have different beam velocity distributions, it is difficult to have the same time-dependent atomic beam intensity distributions for Kr and Xe. As a result, we are not able to obtain the ratio of total cross sections between Kr and Xe.

In conclusion, we demonstrated that the increase of vibrational energy from 16 194 to 18 922 cm^{-1} does not make a significant difference in energy transfer. The energy transfer properties also remain the same when H atoms in naphthalene are replaced by D atoms, indicating that the high vibrational frequency modes do not play important roles in the energy transfer. They are not important in supercollisions either. However, as Kr atoms are replaced by Xe atoms, differences were observed. The changes include the decrease of the probabilities for large V→T energy transfer in the backward direction and the values of maximum V→T energy transfer.

ACKNOWLEDGMENTS

This work was partly supported by the National Science Council, Taiwan, under Contract No. NSC95-2113-M-001. We thank Professor Y. T. Lee and I. Oref for many helpful discussions.

[1] D. C. Tardy and B. S. Rabinovitch, Chem. Rev. (Washington, D.C.) **77**, 369 (1977).
[2] I. Oref and D. C. Tardy, Chem. Rev. (Washington, D.C.) **90**, 1407 (1990).
[3] J. R. Barker, L. M. Yoder, and K. D. King, J. Phys. Chem. A **105**, 796 (2001).
[4] A. S. Mullin, C. A. Michaels, and G. W. Flynn, J. Chem. Phys. **102**, 6032 (1995).
[5] C. A. Michaels, A. S. Mullin, J. Park, J. Z. Chou, and G. W. Flynn, J. Chem. Phys. **108**, 2744 (1998).
[6] E. T. Sevy, S. M. Rubin, Z. Lin, and G. W. Flynn, J. Chem. Phys. **113**, 4912 (2000).
[7] M. C. Wall and A. S. Mullin, J. Chem. Phys. **108**, 9658 (1998).
[8] M. C. Wall, A. E. Lemoff, and A. S. Mullin, J. Chem. Phys. **111**, 7373 (1999).
[9] H. Hold, T. Lenzer, K. Luther, K. Reihs, and A. C. Symonds, J. Chem. Phys. **112**, 4076 (2000).
[10] T. Lenzer, K. Luther, K. Reihs, and A. C. Symonds, J. Chem. Phys. **112**, 4090 (2000).
[11] H. Frerichs, M. Hollerbach, T. Lenzer, and K. Luther, J. Phys. Chem. A **110**, 3179 (2006).
[12] U. Hold, T. Lenzer, K. Luther, and A. C. Symonds, J. Chem. Phys. **119**, 11192 (2003).
[13] D. K. Havey, Q. Liu, Z. Li, M. Elioff, M. Fang, J. Neudel, and A. S. Mullin, J. Phys. Chem. A **111**, 2458 (2007).
[14] H. Hippler, H. W. Schranz, and J. Troe, J. Phys. Chem. **90**, 6158 (1986).
[15] G. Lendvay and G. C. Schatz, J. Chem. Phys. **94**, 8864 (1990).
[16] D. L. Clarke, K. C. Thompson, and R. G. Gilbert, Chem. Phys. Lett. **182**, 357 (1991).
[17] I. Oref, Chem. Phys. **187**, 163 (1994).
[18] V. Bernshtein and I. Oref, J. Chem. Phys. **106**, 7080 (1997).
[19] V. Bernshtein and I. Oref, J. Chem. Phys. **108**, 3543 (1998).
[20] A. Linhananta and K. F. Lim, Phys. Chem. Chem. Phys. **4**, 577 (2002).
[21] A. Linhananta and K. F. Lim, Phys. Chem. Chem. Phys. **2**, 1385 (2000).
[22] C. J. Higgins and S. Chapman, J. Phys. Chem. A **108**, 8009 (2004).
[23] C. J. Higgins, Q. Ju, N. Seiser, G. W. Flynn, and S. Chapman, J. Phys. Chem. A **105**, 2858 (2001).
[24] Z. Li, R. Sansom, S. Bonella, D. F. Coker, and A. S. Mullin, J. Phys. Chem. A **109**, 7657 (2005).
[25] U. Grigoleit, T. Lenzer, K. Luther, M. Mutzel, and A. Takahara, Phys. Chem. Chem. Phys. **3**, 2191 (2001).
[26] U. Grigoleit, T. Lenzer, and K. Luther, Z. Phys. Chemie-Int. J. Res. Phys. Chem. Chem. Phys. **214**, 1065 (2000).
[27] H. Hipper, L. Lindemann, and J. Troe, J. Chem. Phys. **83**, 3906 (1985).
[28] H. Hipper, B. Otto, and J. Troe, Ber. Bunsenges. Phys. Chem. **93**, 428 (1989).
[29] M. Damm, H. Hipper, and J. Troe, J. Chem. Phys. **88**, 3564 (1988).
[30] M. J. Rossi, J. R. Pladziewicz, and J. R. Barker, J. Chem. Phys. **78**, 6695 (1983).
[31] J. Shi, D. Bernfeld, and J. R. Barker, J. Chem. Phys. **88**, 6211 (1988).
[32] J. Shi and J. R. Barker, J. Chem. Phys. **88**, 6219 (1988).
[33] B. M. Toselli and J. Barker, J. Chem. Phys. **97**, 1809 (2002).
[34] C. L. Liu, H. C. Hsu, J. J. Lyu, and C. K. Ni, J. Chem. Phys. **123**, 131102 (2005).
[35] H. C. Hsu, J. J. Lyu, C. L. Liu, C. L. Huang, and C. K. Ni, J. Chem. Phys. **124**, 054301 (2006).
[36] C. L. Liu, H. C. Hsu, J. J. Lyu, and C. K. Ni, J. Chem. Phys. **124**, 054302 (2006).
[37] C. L. Liu, H. C. Hsu, J. J. Lyu, and C. K. Ni, J. Chem. Phys. **125**, 204309 (2006).
[38] C. L. Liu, H. C. Hsu, Y. C. Hsu, and C. K. Ni, J. Chem. Phys. **127**, 104311 (2007).
[39] V. Bernshtein, I. Oref, C. L. Liu, H. C. Hsu, and C. K. Ni, Chem. Phys. Lett. **429**, 317 (2006).
[40] V. Bernshtein and I. Oref, J. Chem. Phys. **125**, 133105 (2006).
[41] V. Bernshtein and I. Oref, Mol. Phys. (unpublished).
[42] C. L. Liu, H. C. Hsu, and C. K. Ni, Phys. Chem. Chem. Phys. **7**, 2151 (2005).
[43] J. J. Lin, J. Zhou, W. Shiu, and K. Liu, Rev. Sci. Instrum. **74**, 2495 (2003).
[44] C. Reyle and P. Brechignac, Eur. Phys. J. D **8**, 205 (2000).
[45] M. Suto, X. Wang, J. Shan, and L. C. Lee, J. Quant. Spectrosc. Radiat. Transf. **48**, 79 (1992).
[46] P. Avouris, W. M. Gelbart, and M. A. El-Sayed, Chem. Rev. (Washington, D.C.) **77**, 793 (1977).
[47] M. Stockburger, H. Gattermann, and W. Klusmann, J. Chem. Phys. **63**, 4529 (1975).
[48] D. L. Clarke, K. C. Thompson, and R. G. Gilbert, Chem. Phys. Lett. **182**, 357 (1991).
[49] H. Hippler, J. Troe, and H. J. Wendelken, J. Chem. Phys. **78**, 6709 (1983).
[50] H. Hippler, J. Troe, and H. J. Wendelken, J. Chem. Phys. **78**, 6718 (1983).